LETTER　　　　## Ecological and conceptual consequences of Arctic pollution

Alexander V. Kirdyanov,[1,2,3] Paul J. Krusic,[1,4] Vladimir V. Shishov,[2,3,5] Eugene A. Vaganov,[2,6] Alexey I. Fertikov,[3] Vladimir S. Myglan,[7] Valentin V. Barinov,[7] Jo Browse,[8] Jan Esper,[9] Viktor A. Ilyin,[5] Anastasia A. Knorre,[3,10] Mikhail A. Korets,[2] Vladimir V. Kukarskikh,[11] Dmitry A. Mashukov,[2] Alexander A. Onuchin,[2] Alma Piermattei,[1] Alexander V. Pimenov,[2] Anatoly S. Prokushkin,[2,3] Vera A. Ryzhkova,[2] Alexander S. Shishikin,[2] Kevin T. Smith,[12] Anna V. Taynik,[7] Martin Wild,[13] Eduardo Zorita[14] and Ulf Büntgen[1,15,16,17]* (iD)

Abstract

Although the effect of pollution on forest health and decline received much attention in the 1980s, it has not been considered to explain the 'Divergence Problem' in dendroclimatology; a decoupling of tree growth from rising air temperatures since the 1970s. Here we use physical and biogeochemical measurements of hundreds of living and dead conifers to reconstruct the impact of heavy industrialisation around Norilsk in northern Siberia. Moreover, we develop a forward model with surface irradiance forcing to quantify long-distance effects of anthropogenic emissions on the functioning and productivity of Siberia's taiga. Downwind from the world's most polluted Arctic region, tree mortality rates of up to 100% have destroyed 24,000 km² boreal forest since the 1960s, coincident with dramatic increases in atmospheric sulphur, copper, and nickel concentrations. In addition to regional ecosystem devastation, we demonstrate how 'Arctic Dimming' can explain the circumpolar 'Divergence Problem', and discuss implications on the terrestrial carbon cycle.

Keywords

Arctic Dimming, boreal forest, Divergence Problem, industrial pollution, Norilsk Disaster, Russia, Siberia, tree rings.

Ecology Letters (2020)

INTRODUCTION

Fifty years after the first 'Earth Day' and nearly half a century after the scientific debate on forest dieback and decline began in Europe and the US (Siccama *et al.*, 1982; Innes, 1987), which generated much social and some political action on global environmental issues (Lewis, 1990), the various direct and indirect effects of industrial pollution on the functioning and productivity of forest ecosystems are still poorly understood (Büntgen *et al.*, 2014). This is particularly true for the boreal forests of the Northern Hemisphere (Gauthier *et al.*, 2015; Girardin *et al.*, 2016), a circumpolar biome that plays a major role in shaping the Earth's carbon cycle and climate system (Bradshaw and Warkentin, 2015). Since the mid-20th century, boreal forests in Eurasia and northern North America have become the dumping ground for large concentrations of anthropogenic air pollutants (McConnell *et al.*, 2007).

Located *c.* 300 km north of the Arctic Circle in central Siberia (69°21'N, 88°11'E), Norilsk is the world's northernmost city with over 100 000 inhabitants. Since the onset of Eurasia's heavy industrialisation in the 1930s, pollution from the Norilsk mining complex (Kharuk et al. 1996) has destroyed vast areas of pristine taiga and tundra habitats on the Taimyr Peninsula (Bauduin *et al.*, 2014; Korets *et al.*, 2014). Experimental metallurgy in Norilsk began as early as 1938 (Table S1), refined nickel production started in 1942, and mining activities have continued to rapidly expand (Dolgikh, 2006). In 2018, the Norilsk complex released *c.* 1 805 200 tons of pollutants (Ministry of Ecology and Environmental Management of the Krasnoyarsk region, 2019), of which *c.* 98% was sulphur dioxide (SO₂), making this taiga region of approximately 24 000 km² the most polluted in the world (Blacksmith Institute and Green Cross Switzerland, 2013). Norilsk's unrestricted emissions of highly noxious substances are not only extremely harmful to humans (Arutyunyan *et al.*, 2014), but also to flora and fauna (Zhulidov *et al.*, 2011; Telyatnikov and Prystyazhnyuk, 2014). The most recent release of more than 20,000 tons diesel oil in the summer of

[1]*Department of Geography, University of Cambridge, Cambridge CB2 3EN, UK*

[2]*V.N. Sukachev Institute of Forest SB RAS, Federal Research Centre, Krasnoyarsk 660036, Russia*

[3]*Institute of Ecology and Geography, Siberian Federal University, Krasnoyarsk 660041, Russia*

[4]*Department of Physical Geography, Stockholm University, Stockholm 106 91, Sweden*

[5]*Mathematical Methods and IT Department, Siberian Federal University, Krasnoyarsk 660075, Russia*

[6]*Rectorate, Siberian Federal University, Krasnoyarsk 660041, Russia*

[7]*Institute of Humanities, Siberian Federal University, Krasnoyarsk 660041, Russia*

[8]*Center for Geography and Environmental Science, University of Exeter, Penryn TR10 9FE, UK*

[9]*Department of Geography, Johannes Gutenberg University, Mainz 55099, Germany*

[10]*State Natural Reserve (Stolby), Krasnoyarsk 660006, Russia*

[11]*Institute of Plant and Animal Ecology, Ural Branch RAS, Ekaterinburg 620144, Russia*

[12]*US Forest Service, Durham, NH 08324, USA*

[13]*Institute for Atmosphere for Climate Science, ETH-Z, Zurich 8092, Switzerland*

[14]*Helmholtz Centrum Geesthacht, Institute of Coastal Research,Geesthacht 21502, Germany*

[15]*Swiss Federal Research Institute WSL, Birmensdorf 8903, Switzerland*

[16]*Global Change Research Centre (CzechGlobe), Brno 603 00, Czech Republic*

[17]*Department of Geography, Faculty of Science, Masaryk University, Brno 613 00, Czech Republic*

Correspondence: E-mail: ulf.buentgen@geog.cam.ac.uk

2020 underlines the growing environmental threat of Norilsk's industrial sector under Arctic warming and permafrost thawing (https://www.bbc.co.uk/news/world-europe-52977740).

Despite the unprecedented level of regional environmental destruction, and the obvious downwind effects of heavy metal pollution, a quantitative assessment of large-scale ecosystem devastation due to airborne pollutants from local emissions has not previously been undertaken. Moreover, there are no reliable measures on the rate and volume of pollutants from lower latitudes that are transported into the Arctic (Law and Stohl, 2007; Arnold *et al.*, 2016). Nevertheless, we know that the highest atmospheric concentration of pollutants occurs in the once pristine and particularly vulnerable ecosystems of northern Siberia (Stohl, 2006; Arnold *et al.*, 2016).

One prominent example of possible ecosystem dysfunction is the 'Divergence Problem' (DP) in dendrochronology: The idiopathic decoupling of tree growth to rising instrumental summer temperatures since around the 1970s (Smith et al., 1999; Briffa *et al.*, 1998; D'Arrigo *et al.*, 2008; Esper and Frank, 2009). Evidence for reduced sensitivity of tree growth to temperature has mainly been reported from forest sites at the high-northern latitudes. This alleged circumpolar phenomenon describes the apparent inability of formerly temperature sensitive tree-ring width (TRW) and maximum latewood density (MXD) chronologies to parallel the recent increase of instrumental temperature measurements. In addition to such low-frequency trend offset, some boreal sites indicate a failure of previously temperature-driven tree growth to reflect high-frequency, summer temperature signals in a warming world. Suggested explanations include drought stress, changes in stratospheric ozone concentration, non-linear growth-climate response, insufficient instrumental climate data for proxy calibration, as well as methodologically induced pitfalls associated with chronology development. Thus far, the causes, scale and consequences of the DP remain unknown (see Vaganov *et al.*, 1999; Kirdyanov *et al.*, 2003; Wilmking *et al.*, 2005; Driscoll *et al.*, 2005; Lloyd and Bunn, 2007; Pisaric *et al.*, 2007; Büntgen *et al.*, 2008, 2009; D'Arrigo *et al.*, 2008; Esper and Frank, 2009 for further details). The DP therefore continues to cast a serious concern on the reliability of high-latitude tree ring-based temperature reconstructions. Despite some pioneering work by Stine and Huybers (2014), little to no attention has been paid to the role of anthropogenic air pollutants and/or atmospheric dimming to explain the DP. Moreover, forward modelling of tree growth under different pollution scenarios has never been applied systematically in pursuit of understanding the DP.

Here, we utilise hundreds of TRW samples from living and dead conifers surrounding the Norilsk industrial complex to reconstruct the sequence of events leading up to a historically unprecedented forest dieback and decline, in one of the world's most polluted regions, since the 1930s. We expand our dendrochronological findings with high-resolution measurements of wood and soil chemistry to quantify the spatiotemporal extent of Norilsk's devastating ecosystem damage. We develop a process-based forward model of boreal tree growth to detect and attribute the effects of changes in surface solar radiation (see Büntgen *et al.*, 2020 for the methodological and conceptual extension of 'Detection & Attribution' to global change ecology). Considering reduced surface irradiance as a proxy for anthropogenic air pollutants, we find strong evidence to suggest 'Arctic Dimming' (AD) has substantially reduced tree growth since *c.* 1970. Similar to 'Global Dimming' (Wild, 2009), AD refers to a decrease in surface solar radiation in the second half of the 20th century, which is in line with independent long-term observations of sunshine duration, diurnal temperature range, pan evaporation, and, more recently, also satellite-derived estimates (Stanhill, 2005; Wild, 2016). In addition to major practical implications, reduced solar radiation at the Earth's surface affects a large number of processes, including evaporation and associated hydrological components, snow and glacier melt, plant photosynthesis and related terrestrial carbon cycle dynamics, as well as the diurnal and seasonal course of surface temperatures (see Wild, 2009, 2016 for a review of changes in surface solar radiation). Causes for AD can either be external, such as changes in the amount of solar radiation incident on the planet at the top of the atmosphere, or internal, such as changes in the transparency of the atmosphere that modify the solar beam on its way to the Earth's surface. Aerosols and clouds, which are not independent from each other (Ramanathan *et al.*, 2001), have been considered the most likely factors for AD, and it is important to note that aerosols affect clouds in different ways depending on the levels of air pollution. Associated with anthropogenic pollution, aerosols can directly modify surface solar radiation by scattering and/or absorbing solar radiation in the atmosphere depending on their composition. Furthermore, aerosols can modify surface solar radiation indirectly through their ability to act as cloud condensation nuclei, thereby altering cloud optical properties and lifetime. As a semidirect effect, absorbing aerosols in heavily polluted regions are also known to heat and stabilise the atmosphere, which may inhibit cloud formation or dissolve existing clouds. In summary, all these factors and processes trigger dimming with increasing aerosol levels in the atmosphere (Wild, 2009), which are considered particularly high in the Arctic (Law and Stohl, 2007; Flanner, 2013; Stohl *et al.*, 2013; Arnold *et al.*, 2016).

MATERIALS AND METHODS

Dendroecology

To characterise the direct, downwind impact of airborne emissions from the Norilsk industrial complex on forest ecosystems, eight dendrochronological sites were established along a northwest-to-southeast transect through zones of different pollution levels (Fig. 1; Tables S2–S3). Across most of this transect, Siberian larch (*Larix sibirica* Ledeb.) is the main forest-forming species. At the southern end of the transect, Siberian spruce (*Picea obovata* Ledeb.) is intermixed with larch. The trees at site 1, located 50 km west of Norilsk, do not exhibit any visual evidence of damage or mortality due to the direct effect of pollution. At site 2, located 28 km west of Norilsk, the forest may be characterised as having *c.* 50% mortality, but at sites 3–7 the degree of tree mortality increases to 100%. At site 8, the south-eastern most location 85 km from Norilsk, *c.* 25% of larch and *c.* 90% of spruce trees were still alive when sampled.

Sites 1–4 were sampled in 2014 and 2015, and at sites 5–8, samples were collected in 2004. All eight sites may be described as open stands within the context of a forest-tundra ecosystem. At sites 2–8, sub-plots 1–3 of *c.* 0.15–0.2 ha were established where, in addition to core and disk samples, measurements of slope and exposure were also taken. At least 30 trees were sampled at each sub-plot. Located outside of the direct influence of Norilsk's pollutants (Fig. 1), site 1 is considered the control/reference site, where only living dominant and co-dominant trees were cored at 1.3 m from the ground. Within the affected sites (2–8), both discs and increment cores were collected from every dead and living tree in each sub-plot at the same height. For each core or disc sample, TRW

was measured at a resolution of 0.01 mm using a LINTAB measuring system (Rinntech-Metriwerk GmbH, Heidelberg, Germany). Depending on the integrity of discs, TRW was measured along multiple radii, including the longest radius (most annual rings), as well as the radius with the widest outermost rings. All TRW series were visually cross-dated and then averaged. To determine when a tree died, the TRW series from standing dead trees were cross-dated against distant site chronologies of similar species considerably south and west of Norilsk and presumed to be unaffected by Norilsk's pollution plume while within the same dendro-climatic zone (Vaganov *et al.*, 1996; Zubareva *et al.*, 2003; Knorre *et al.*, 2006; Kirdyanov *et al.*, 2014). The year of tree death was defined as the
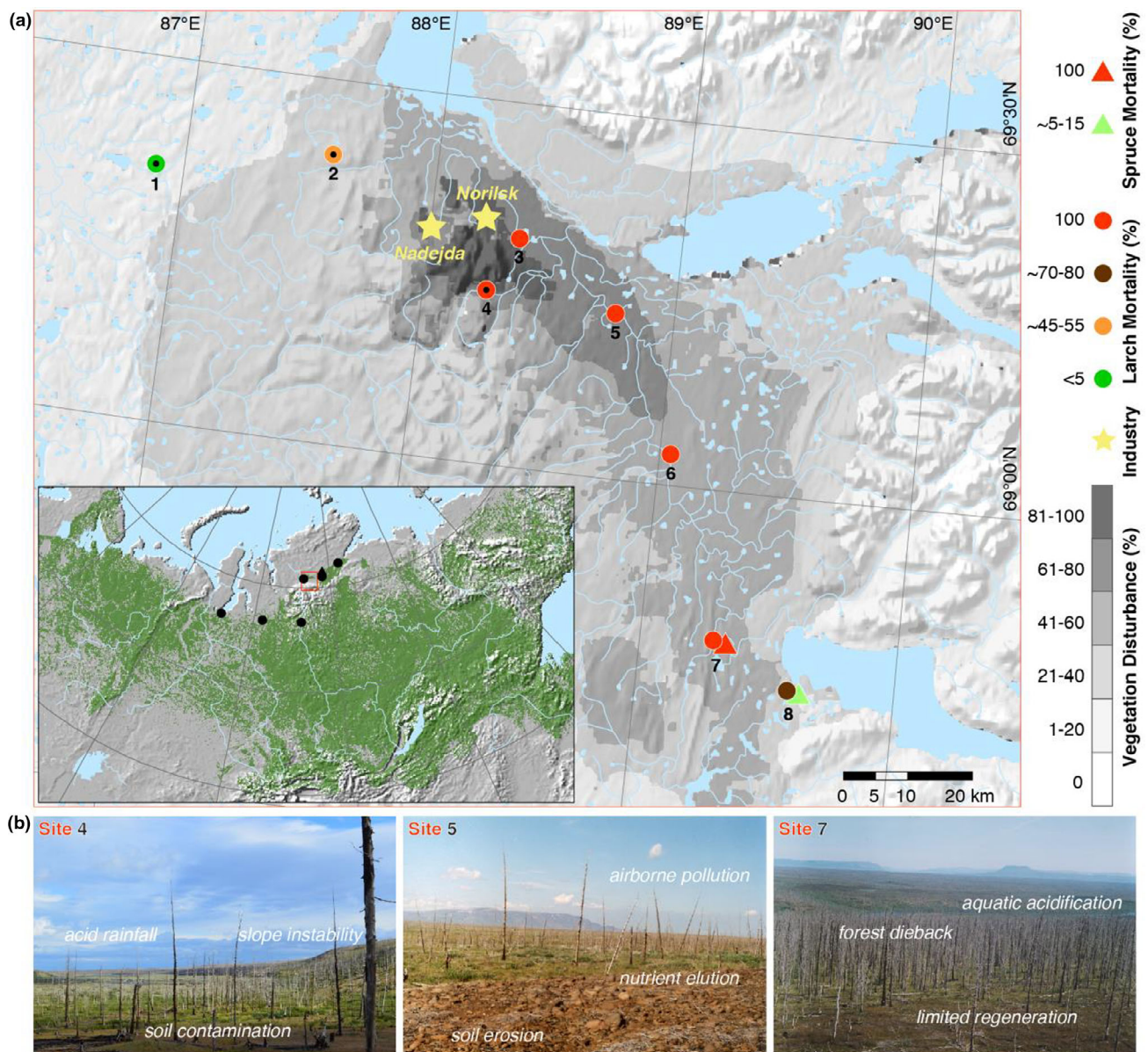

Figure 1 Environmental devastation. (a) Larch and spruce sampling sites (dots and triangles, respectively) superimposed on different levels of vegetation degradation (grey shadings). Dots with black centres refer to the three sites for which wood chemistry was measured. The red frame in the inset map places the wider Norilsk study region in the context of Russia's boreal forest zone (green area). Black dots (larch) and one triangle (spruce) in the boreal inset map show non-polluted reference sites that have been used in the larger-scale, process-based forward modelling experiment. (b) The three pictures represent different levels and aspects of ecosystem disturbance.

next calendar year following the date of the outermost tree ring.

The number of larch and spruce trees analysed per site varied from 12 to 106 (Table S3). To estimate the pollution effect on radial tree growth, we developed TRW chronologies for each site. Depending on the course of the raw TRW measurements, we either fitted negative exponential functions, horizontal lines, or cubic smoothing splines with 50% frequency-response cut-off equal to 2/3 of the individual series length. We then divided the observed values by their associated curve values, thereby transforming each raw TRW series into a new timeseries of dimensionless indices (Cook and Peters, 1997). The final TRW chronologies were produced by computing the robust mean of the index TRW series from all trees per site (Fritts, 1976). To estimate possible effects of pollution on tree growth for regions not directly impacted by Norilsk's emissions, we used a recently developed collection of *Larix sibirica*, *Picea obovata* and *Larix gmelinii* TRW chronologies from seven sites along a >1400 km long east-west transect that extends considerably south and west of Norilsk (Fig. 1; Table S4). These contributed chronologies share a significantly high degree of growth coherency (Table S5), permitting the use of their average as an expression of large-scale mean, boreal forest growth.

Wood and soil chemistry

The sulphur (S), copper (Cu) and nickel (Ni) content of the wood samples from sites 1, 2 and 4, locations that represent different levels of pollution exposure, was measured by X-ray fluorescence (XFR) with an Itrax Multiscanner (Cox Analytical Systems, Sweden). From each of the three sites, between six and eight wood samples without obvious defects or decay were chosen for this analysis. Wood laths of 2 mm thickness cut from the discs or cores were exposed to high intensity X-ray beams. Light and heavy elements were detected with an X-ray tube fitted with a Cr and a Mo anode, respectively, and operated at 30 kV and 50 mA. Each sample lath was irradiated for 10 s at 100-μm intervals along the sample core or disc sample radius. The XRF energy emitted from the excited sample surface was continuously recorded by a silicon drift chamber detector (SDD). Peaks in the continuous XRF spectrum were assigned to specific elements using the Q-spec software (Cox Analytical Systems, Sweden). Relative concentrations (i.e. count rates of fluorescent photons) for the pre-defined S, Cu and Ni elements were obtained at every measurement point. A dedicated FORTRAN program was written to align and integrate the continuous 100 μm elemental fluorescent counts with the incremental measurements taken along the same path as the XRF measurements in order to produce annual count values of S, Cu and Ni.

The topsoil S, Cu and Ni content was measured in 3–4 soil samples taken from the upper organic-rich layer at those TRW sampling sites where the wood chemistry was also measured. That is at the reference site 1, as well as the pollution-affected sites 2 and 4 (Table S2). Prior to the chemical analyses, each of the soil samples was air dried, sieved through a 1 mm mesh size, and milled down to 0.074 mm in grain size. Bulk elemental content was determined by means of XRF

analysis with a MobiLAB X-5000 scanner (OLYMPUS Innov-X, USA). The fluorescence values were calibrated against geochemical standards provided by the Vinogradov Institute of Geochemistry SB RAS (Irkutsk, Russia). We created a GIS database of spatially referenced geographic, topographic and vegetation data from both remote sensing platforms and ground surveys for the Norilsk industrial region (see supporting online information for details). Different disturbance levels were used for vegetation classification and mapping (Table S6).

Forward modelling

The Vaganov-Shashkin model (VS-model) is a process-based forward model that simulates TRW as a function of climate (Vaganov *et al.*, 2006, 2011). The full, high-resolution VS-model requires daily air temperature, soil moisture, and solar radiation as input variables. However, as long-term daily climate data for our research region are unavailable, we used the VS-Lite variant, a simplified version of the VS-model that accepts monthly temperature and precipitation data (Tolwinski-Ward *et al.*, 2011, 2013), which exist from 1901 to 2018 (CRU TS4.01; Harris *et al.*, 2014). The VS-Lite model calculates the monthly rate of TRW formation Gr that is determined as the minimum of two partial growth rates: The growth rate that is dependent on temperature (Gr_T) and the rate that is dependent on moisture (Gr_W), multiplied by the growth rate influenced by solar radiation (Gr_E) at a given latitude and month m of the year y (Evans *et al.*, 2006). The simulated TRW series are obtained by integrating the growth response function $Gr(m,y)$ over a variable window of months defined by the monthly start and end parameters (I_0 and I_f). Parameterisation of the model aims to find the best fit between the simulated TRW, normalised with respect to their 1901–1942 values, and a target TRW chronology, the average of the above-mentioned *L. sibirica*, *P. obovata* and *L. gmelinii* chronologies, by adjusting the values for the 12 site parameters in the VS-Lite model that tune the model to local conditions (Tychkov *et al.*, 2019). The solution to tuning the model by direct mathematical optimisation of the multidimensional parameter space is problematic due to a high probability of reaching the local optimum that generates an artificial decision (Etschberger and Hilbert, 2003; Borg and Mair, 2017). The value for any one parameter values should not conflict with the biological constraints on growth and/or site conditions observed in the field data.

We used a specially developed optimal estimation of 12 basic model parameters from the differential evolution (DE) approach (Storn and Price, 1997; Price *et al.*, 2005) in the R-code version of the VS-Lite model (Table S7). This approach finds the optimal values for multidimensional real-valued function or mathematical system of the functions. DE does not use the gradient of the problem being optimised, which means DE does not require the parameter optimisation to be differentiable, as is required by classic optimisation methods such as gradient descent and quasi-Newton methods. Therefore, DE can be applied to a wide class of the process-based models. Optimal values of the VS-Lite parameters obtained by the DE are considered as a vector that contains highly

significant positive Pearson's correlation coefficients ($P < 0.01$), and minimises the root mean square error (RMSE) between simulated TRW curves and the target dendrochronology over independent calibration (1901–1942) and verification (1943–2015) periods. Adopted to the VS-Lite parameterisation module, the DE approach was tested on a server Supermicro SYS-2028GR-TR (64 cores on Intel Xeon E5-2698 processors, 256 GB of ESS RAM). To obtain optimal parameter estimations, we began with 120 optimal sets of the model parameters and selected a decision (optimal set), which provides the best simulation fit of the observed TRW chronology due to the criteria described above.

Surface radiation

We assume the level of total (R_s) and photometrically active (PAR) solar radiation reaching the surface depends on the transparency of the atmosphere, which is related to the amount and structure of daily cloud cover that in turn may be related to the amount of air pollution in the local atmosphere (Shindell, 2007; Najafi *et al.*, 2015; Acosta Navarro *et al.*, 2016). Anthropogenic, as well as natural formed aerosols can enhance the formation and residence time of clouds particularly in relatively pristine regions such as the Arctic (Wild, 2009, 2016). We assume that current trends in atmospheric transparency are mainly driven by air pollution, punctuated every now and then by volcanic eruptions, and that these pollutants have both direct and indirect effects on clouds (Roderick and Farquhar, 2002; Wild, 2009; Malavelle et al., 2017), and clouds inversely modulate the diurnal temperature range (DTR). We assume, as an approximation, a linear relationship between variations in DTR and variations in cloud cover, the latter including the effect of aerosols. This link between DTR and cloud cover has been shown to be valid for timescales from month to decade (Wild *et al.*, 2007; Wild, 2009; Wang and Dickinson, 2013), for which R_s is highly correlated with PAR ($r = 0.97$, $n = 14667$, $P < 10^{-8}$). The long-term DTR was used as a proxy for R_s (PAR) over 1901–2018. For the study region, a change in R_s by $1\ Wm^{-2}$ leads to changes in DTR by 0.02–0.04°C (Wang and Dickinson, 2013).

The gridded CRU TS v. 4.02 (Harris *et al.*, 2014) DTR data were used to obtain low-pass frequency variations of R_s over our region of interest. The averaged summer (June–August) DTR, from all grid cells, was smoothed with a 21-year Gaussian low pass filter (Wild *et al.*, 2017), and R_s was obtained for each year y according to the following equation: $R_s(y) = DTR(y)/_\delta$ where $DTR(y)$ represents the value of smoothed DTR in year y; δ is a temperature coefficient that is allowed to vary from 0.02 to 0.04°C. We considered δ as a proxy parameter of the model (see Table S7), which was involved in the DE procedure. In our experiments, the best results were found for R_s corresponding to changes in DTR at a rate of 0.03 °C per $1\ Wm^{-2}$. Finally, the normalised (Basheer and Hajmeer, 2000) low-pass radiation R_s for each year y is multiplied by the $Gr_E(m,y)$ and used in the VS-Lite model. It is important to note that TRW simulations performed with the effect of AD ($R_{s(y)}$) derived from regional reanalysis solar radiation data (Compo *et al.*, 2011) did not produce satisfactory results.

RESULTS

Here, we report on 88 724 annually resolved and absolutely dated TRW and wood chemistry measurements from 46 living and 503 dead Siberian larch and spruce trees that grew at eight sites along a *c*. 150 km northwest-to-southeast transect through the Norilsk complex (Fig. 1a). Each site represents a different pollution exposure level due to dispersal effects of the prevailing westerly winds (Table S2). The mean age of the analysed larch and spruce trees ranges from 71 to 216 years, with minimum and maximum ages 31–113 and 214–388 years, respectively. Varying from 0.31 to 0.84 mm, the site-specific, average annual radial stem growth rates are slightly lower for spruce than for larch (Table S3). A 45-day-long polar night, annual mean temperatures of circa −10°C, and daily cold extremes of up to −50°C that can occur from September to May (based on meteorological measurements at Dudinka, 1906–2012), constrain tree growth to just a few weeks between June and August.

The first year of larch decline leading to tree mortality coincides with the first year of smelter operation (Fig. 2a). Although tree mortality south-east of Norilsk started as early as 1938, the annual dieback rates of up to 5% remained relatively low at sites 3 and 4 until the 1960s. Mortality increased to 30% per year at site 4 in the second half of the 1960s, when the 'Mayak' mine opened and SO$_2$ emissions escalated (Table S1). By the early 1980s, all larch trees within 69 km east-southeast of Norilsk had died at sites 3–7, and at site 8 by the time of this reporting, only about 25% of the larch trees have survived. Protected from the dominant westerly airflow, site 1 and 2 west of Norilsk are less affected (Figs 1 and 2a). Forest dieback at site 2 gradually tracks SO$_2$ deposition until the 'Nadejda' complex started operation, after which dieback rapidly increased. Built in 1979, this latest smelter reached full capacity in the early 1980s, at which time Norilsk's heavy metal production grew five-fold. By 1983, Norilsk's annual industrial emissions peaked at 2 483 000 tons (Kharuk et al. 1996). Spruce dieback at site 7 started in the 1970s, about a decade after the larch decline, whereas at the furthermost site 8, spruce mortality rates of only 10% were reached as late as the 2000s (Fig. 2a). Almost all of the surviving conifers in the study area exhibit heavy crown damage, and the comparison of TRW near Norilsk with observations of regional summer temperature variability suggests an unprecedented decoupling in the second half of the 20th century (Fig. 2b). While TRW variations parallel June–August temperature means fairly well until around 1970 ($r = 0.42$, $P < 0.01$ for 1924–1969), the overall low growth rates of the surviving trees clearly depart from the recent warming afterwards ($r = 0.02$, $P > 0.05$ for 1970–2015).

The wood chemical analyses reveal a significant rise in S, Cu and Ni in all larch samples from site 4 (Fig. 3), with peak values during the late 1960s. Although the chemical profiles vary among individual trees, the elemental-specific patterns of site 4 exhibit a coherent picture of exposure to airborne pollution from Norilsk. Sulphur levels slowly start to increase in the 1930s, but do not significantly rise until the mid-1950s. Copper rises from background levels in the 1940s to peak concentrations in the mid-1960s. In contrast, none of the
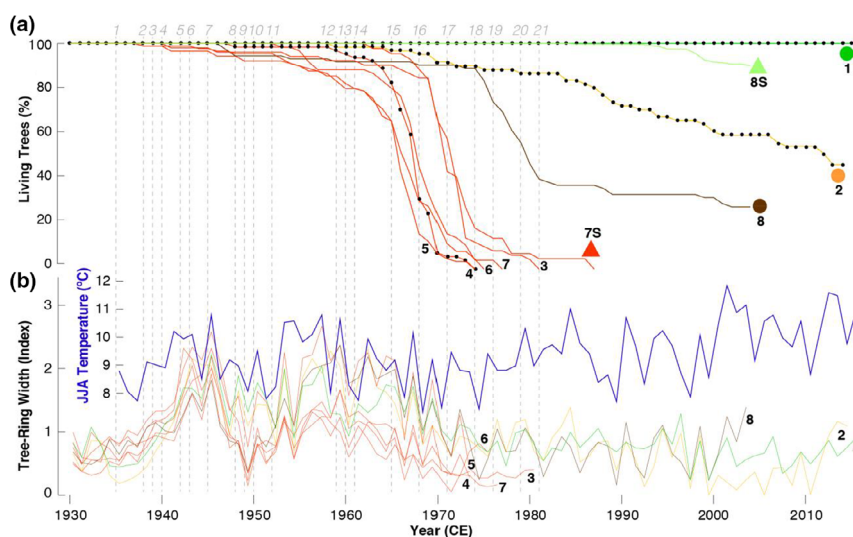
Figure 2 Forest dieback. (a) Percentage of dead trees per site relative to the total number of living trees in 1930 CE, with site codes, colours and symbols corresponding to Figure 1. Solid lines refer to the three sites for which wood chemistry was measured. (b) Standardised larch TRW chronologies from Norilsk, together with June–August (JJA), near-surface summer temperature means from the CRU TS4.01 grid box over our study area (87–90 °E and 68–71 °N). Dashed vertical lines, coded with light grey numbers, refer to the beginning of main industrial developments: 1 = first electric power station; 2 = first experimental 1.5 t of high-grade Ni-Cu matte; 3 = small metallurgical plant; 75 t of Ni-Cu low-grade matte; 4 = first experimental factory for concentrating; 5 = first nickel factory, as well as electric power and heat station; 6 = first electrolyte Ni production; 7 = significant production increase; 8 = first coke oven battery; 9 = first Cu factory; 10 = first Cu electrolysis shop, plus first brick, cement and lime factories; 11 = first metallurgical shop; 12–14 = modernisation of Ni factory; 13,15 = discovery of particularly S-rich ore deposits at Talnakh and Oktyabr'skoye; 15–19 = first mining of S-rich deposits; 20 = first production of Nadejda; 21 = full operation of Nadejda (see Table S1 for details).

living trees from the 'unpolluted' reference site 1 show similar chemistry values (Fig. 3). However, substantial increases in S, Cu and Ni are found in the outermost rings of most of the dead larches at site 2. Spatiotemporal variation in the chemical concentration of the tree rings is corroborated by independent S, Cu and Ni measurements in the upper organic soil layer at each of the three sites (1, 2 and 4). The highest topsoil pollution is found at site 4 in 2014 (Table S2), when S, Cu and Ni concentrations peak at 2,660 ($\pm$188), 828 ($\pm$85) and 716 ($\pm$29) mg/kg (SD) respectively. The lowest soil contamination is found at site 1 (S = 359 ($\pm$27), Cu = 33 ($\pm$7) and Ni = 36 ($\pm$7) mg/kg). The medium level of soil pollution at site 2 agrees with the chemical concentrations found in the wood at the same site, consistent with the predominant west-northwest airflow that disperses polluting aerosols from Norilsk.

While trees in the vicinity of Norilsk have died of continuous exposure to uncontrolled industrial emissions since the 1940s, trees growing outside the area directly impacted by Norilsk's industrial pollutants are suffering. Reduced growth rates across the boreal forest since around the 1970s are indicative of the DP and beg the question 'what is hampering tree growth?'. To assess the putative large-scale, long-term effects of industrial pollution on the vigour of Siberia's taiga, we compared the rates of tree growth from the VS-Lite model to those empirically derived from seven sites sufficiently far away from Norilsk that can be considered free from the obvious direct effects of industrial pollution (Fig. 1 insert; Table S4). The VS-Lite model reproduces the measured TRW until *c.* 1970 (Fig. 4a), after which the simulated and measured growth rates increase and decrease, respectively. While

simulated and measured TRW during the 1901–1942 pre-industrial period is highly synchronous, correlation between the simulated TRW chronology and the measured TRW chronology is insignificant afterwards ($P > 0.05$). This obvious divergence between increasing simulated and decreasing measured TRW suggests the existence of a spatially extensive, negative forcing capable of dramatically countering the beneficial effects of the recent warming trend. After reducing incoming surface solar radiation (i.e. implementing dimming), the simulated TRW parallels the observed growth rates over the entire 20th century and until 2018 (Fig. 4b; Tables S8). Correlations between simulated and measured TRW are now highly significant from 1901 to 2018 ($P < 0.0001$). After 10-year low-pass filtering, the measured TRW chronology correlates with the simulated TRW data (without dimming) at 0.48 and −0.38 over the 1901–1969 and 1970–2018 periods respectively (Fig. 4b). Both values, and particularly the later one, significantly increase to 0.62 and 0.79 when dimming is incorporated into the VS-Lite model.

DISCUSSION

Although Norilsk is an extreme example of industrial pollution, it is not atypical for the high-northern latitudes that are more polluted than anticipated (Arnold *et al.*, 2016). Since the mid-20th century, continuous SO_2 emissions from high-latitude mining, oil and shipping activities (Fig. S1; Table S9) have affected biogeochemical cycles not only over central and eastern Siberia (Shevchenko *et al.*, 2003), but also across much of the circumpolar Arctic (Hirdman *et al.*, 2010; Bauduin *et al.*, 2014; Panyushkina *et al.*, 2016). Moreover, the
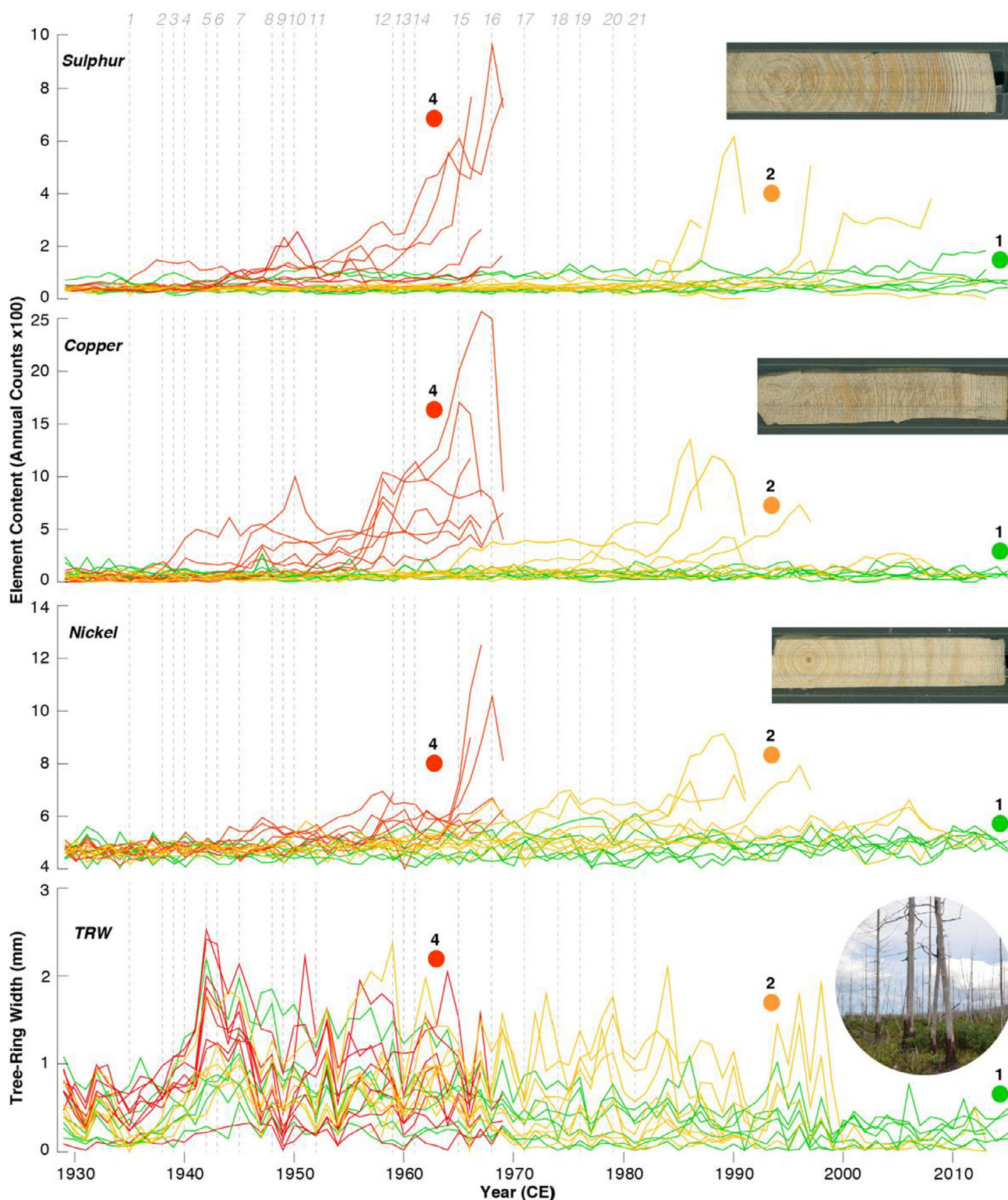
Figure 3 Industrial pollution. Interannual variability in sulphur, copper and nickel (S, Cu and Ni) content of individual tree rings from the low contamination site 1 (green), the medium contamination site 2 where 50% of the trees are dead (yellow) and the high contamination site 4 where all trees are dead (red). The corresponding tree-ring width (TRW) measurements are shown in bottom panel. Site codes, colours and symbols, as well as the vertical dashed lines are as for Figure 2.

high-northern latitudes have long been impacted by transported pollutants, including detailed reports of 'Arctic Haze' events since 1883 (Garrett and Verzella, 2008). 'Arctic Haze'

results from the strong inversion often referred to as the 'Polar Dome' (Stohl, 2006). This circulation pattern is typical of the wintertime Arctic boundary layer, which facilitates
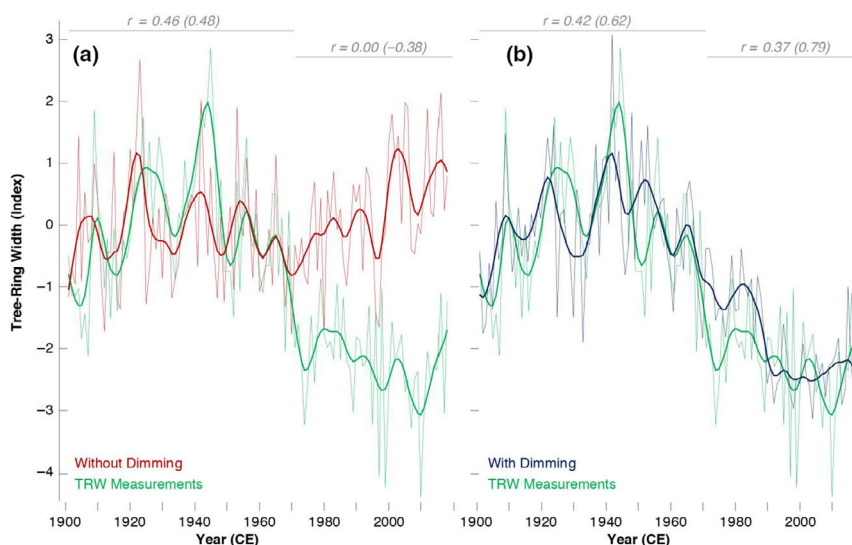
Figure 4 Explaining the 'Divergence Problem' (DP). Measured (green) and simulated boreal tree-ring width (TRW) indices (a) without and (b) with considering large-scale effects of 'Arctic dimming' (AD) in the process-based forward model (VS-Lite). Thick curves are 10-year cubic smoothing splines, and the correlation coefficients between the original (and smoothed) measurements and simulated values refer to the 1901–1969 and 1970–2018 periods.

transportation and accumulation of air pollutants from lower latitudes into the Arctic (Stohl, 2006; Arnold *et al.*, 2016). Unprecedented concentrations of pollutants (McConnell *et al.*, 2007; Smith *et al.*, 2011) have driven both historic cooling and amplified recent warming in the Arctic (Acosta Navarro *et al.*, 2016). Transport from lower latitude Asia and Eurasia increases their content in the upper atmosphere, whereas local emissions of aerosols substantially affect the transparency of the atmosphere and the formation and structure of clouds (Stohl *et al.*, 2013; Zhao and Garrett, 2015). These have been shown to curtail surface irradiance and to cause light diffusion (Stine and Huybers, 2014), with the strongest impact over central and eastern Siberia, as well as parts of Alaska and Canada (Briffa *et al.*, 1998). In addition to the antagonistic role of anthropogenic pollutants, the net primary productivity of the boreal biome is also vulnerable to other abiotic stressors (Beck *et al.*, 2011; Gauthier *et al.*, 2015; Girardin *et al.*, 2016; Charney *et al.*, 2016), such as the redistribution of nitrogen as a consequence of widespread wildfires that are expected to increase in frequency and intensity under future climate change (Ponomarev et al. 2018; Shvetsov *et al.*, 2019; Knorre *et al.*, 2019; Kirdyanov *et al.*, 2020).

The most important Eurasian boreal forest species, larch and spruce, exhibit different leaf morphologies and survival strategies. The deciduous larch habit minimises winter desiccation, whereas evergreen spruce develops thick cuticle to reduce foliar water loss (Miranda and Chaphekar, 1980). The thickened spruce cuticle may also afford greater protection from foliar leaching due to the deposition of acidic pollutants. Since larch foliage has a greater specific leaf area, higher stomatal conductance and lower water use efficiency than spruce (Kloeppel *et al.*, 1998), it might be particularly sensitive to ozone damage (Wieser *et al.*, 2013). Finally, there is reason to believe that boreal tree growth will suffer from reduced nitrogen uptake as regional humidity increases and the vapour pressure deficit decreases (Lihavainen *et al.*, 2016).

Consequently, the expected large-scale ecosystem disturbance due to anthropogenic warming will have serious implications for the Earth's climate system and carbon cycle.

Based on regional- to large-scale modelling, we now suggest that the recent failure of formerly temperature-sensitive boreal tree growth to track increasing instrumental summer temperatures can be attributed to reduced incoming surface solar radiation (Stine et al. 2014; Arnold *et al.*, 2016; Wild, 2016). This finding is consistent with our understanding of the widespread 'Arctic haze' phenomenon (Law and Stohl, 2007), which has been observed since the beginning of the 20th century (Garrett and Verzella, 2008), and has been described as a key driver of AD. We interpret these results as a consequence of reduced solar radiation, attributable to increasing aerosol concentrations (Quinn *et al.*, 2007) due to elevated industrial emissions since the 1930s both emitted in and transported to the Arctic (Law and Stohl, 2007). This assumption is supported by the temporal agreement between the evolution of the DTR and industrial emissions: Both were low before the mid-20th century (McConnell *et al.*, 2007), then in the early-1970s DTR and industrial emissions started to simultaneously display clear parallel trends. The link between industrial emissions and surface solar radiation may be direct (Rinke *et al.*, 2004), or may be mediated by the effects of aerosols on cloud cover and cloud residence time through their impact on condensation nuclei and droplet size (Twomey, 1977; Ramanathan *et al.*, 2001). Long-term changes in cloud cover may be also associated with an increase in atmospheric concentrations of greenhouse trace gases or changes in sea-ice cover (Taylor *et al.*, 2015). At high latitudes, future scenario simulations (Trenberth and Fasullo, 2009) indicate that a stronger greenhouse forcing leads to greater cloud cover. Greenhouse trace gases, therefore, would reinforce the effect of aerosol emissions on cloud cover at high latitudes. However, disentangling the effects of increased greenhouse trace gases from AD remains subject to large uncertainties as aerosol-cloud

interactions and greenhouse-cloud feedbacks are difficult to simulate in climate models, and Arctic aerosol-cloud interactions are not fully understood (Browse *et al.*, 2014). The lack of spatially explicit measurements of air pollutants, cloud cover and solar irradiance during the first half of the 20th century from northern North America, Russia and China, does hinder these modelling analyses.

In conclusion, our study represents, for the first time ever, the combined evidence from dendroecology, biogeochemistry and process-based forward modelling to address the direct and indirect effects of industrial pollution on the functioning and productivity of boreal forest ecosystems at varying spatiotemporal scales. In addition to the quantification of the exceptional rate of environmental devastation around Norilsk, the world's most polluted Arctic region, we demonstrate that anthropogenic-induced AD can explain the yet unresolved DP in tree-ring research. By doing so, we provide an important seal of the quality for any tree ring-based temperature reconstruction, because the Principle of Uniformity as it applies, *sine qua non*, to dendroclimatology and thus to a substantial part of high-resolution palaeoclimatology, remains intact. Our findings are expected to generate widespread environmental and political interest, because we add a unique perspective to the extraordinary level of persistent Arctic pollution, for which scientific and governmental awareness is still lacking. Deeper insights into the effects of long-term industrial emissions on the functioning and productivity of forest ecosystems across the high-northern latitudes further improve understanding of large-scale climate dynamics and changes in the global carbon cycle. This study appears particularly timely in the light of Norilsk's unprecedented release of more than 20,000 tons diesel oil in 2020; an environmental disaster that emphasises the threat of Norilsk's industrial sector under rapid Arctic warming and permafrost thawing, and also stresses the ecological vulnerability of the high-northern latitudes.

AUTHORSHIP

UB, AVK and EAV designed the study. AVK, AIF, AVP, ASS and VVK collected field data. AVK, VSM, AIF, AAK, VVB, AVT, DAM and ASP performed soil chemistry and dendrochronology. MAK, VAR and AAO produced forest disturbance maps. VVS and VAI developed the forward model. AVK, PJK and UB analysed data. JE, JB, AP, KTS, MW and EZ contributed to interpretation and discussion. UB and AVK wrote the paper with input from PJK, JE, JB, VVS and KTS. Each author provided critical discussion and approved submission.

PEER REVIEW

The peer review history for this article is available at https://publons.com/publon/10.1111/ele.13611.

DATA AVAILABILITY STATEMENT

Data available from the Dryad Digital Repository: https://doi.org/10.5061/dryad.tmpg4f4wq

REFERENCES

Acosta Navarro, J.C., Varma, V., Riipinen, I., Seland, Ø., Kirkevåg, A., Struthers, H. *et al.* (2016). Amplification of Arctic warming by past air pollution reductions in Europe. *Nat. Geosci.*, 9, 277–281.

Arnold, S.R., Law, K.S., Brock, C.A., Thomas, J.L., Starkweather, S.M., von Salzen, K. *et al.* (2016). Arctic air pollution: Challenges and opportunities for the next decade. *Elementa*, 4, 000104.

Arutyunyan, R.V., Vorobieva, L.M., Panchenko, S.V., Bakin, R.V., Novikov, S.M., Shashina, T.A. *et al.* (2014). Comparative analysis of radiation and chemical risks to public health in Krasnoyarskiy Kray. *Radiation Risk*, 23, 123–136.

Basheer, I.A. & Hajmeer, M. (2000). Artificial neural networks: fundamentals, computing, design, and application. *J. Microbiol. Methods*, 43, 3–31.

Bauduin, S., Clarisse, L., Clerbaux, C., Hurtmans, D. & Coheur, P.-F. (2014). IASI observations of sulfur dioxide (SO_2) in the boundary layer of Norilsk. *J. Geophys. Res. Atmos.*, 119, 4253–4263.

Beck, P.S.A., Juday, G.P., Alix, C., Barber, V.A., Winslow, S.E., Sousa, E.E. *et al.* (2011). Changes in forest productivity across Alaska consistent with biome shift. *Ecol. Lett.*, 14, 373–379.

Blacksmith Institute, Green Cross Switzerland (2013). The world's worst 2013: The top ten toxic threats. Cleanup, Progress and Ongoing Challenges. Blacksmith Institute, New York.

Borg, I. & Mair, P. (2017). The choice of initial configurations in Multidimensional Scaling: local minima, fit, and interpretability. *Austrian J. Stat.*, 46, 19–32.

Bradshaw, C.J.A. & Warkentin, I.G. (2015). Global estimates of boreal forest carbon stocks and flux. *Glob. Planet. Change*, 128, 24–30.

Briffa, K.R., Schweingruber, F., Jones, P., Osborn, T.J., Shiyatov, S.G. & Vaganov, E.A. (1998). Reduced sensitivity of recent tree-growth to temperature at high northern latitudes. *Nature*, 391, 678–682.

Büntgen, U., Frank, D.C., Wilson, R., Career, M., Urbinati, C. & Esper, J. (2008). Testing for tree-ring divergence in the European Alps. *Glob. Change Biol.*, 14, 2443–2453.

Büntgen, U., Wilson, R., Wilmking, M., Niedzwiedz, T. & Bräuning, A. (2009). The 'Divergence Problem' in tree-ring research. *TRACE*, 7, 212–219.

Büntgen, U., Tegel, W., Kaplan, J.O., Schaub, M., Hagedorn, F., Bürgi, M. *et al.* (2014). Placing unprecedented recent fir growth in a European-wide and Holocene-long context. *Front. Ecol. Environ.*, 12, 100–106.

Büntgen, U., Johnson, D., Gonzalez-Rouco, J.F., Luterbacher, J. & Stenseth, N.C. (2020). Extending the climatological concept of 'Detection and Attribution' to global change ecology in the Anthropocene. *Functional Ecol.*, 1–13. https://doi.org/10.1111/1365-2435.13647

Browse, J., Carslaw, K.S., Mann, G.W., Birch, C.E., Arnold, S.R. & Leck, C. (2014). The complex response of Arctic aerosol to sea-ice retreat. *Atmos. Chem. Phys.*, 14, 7543–7557.

Charney, N.D., Babst, F., Poulter, B., Record, S., Trouet, V.M., Frank, D. *et al.* (2016). Observed forest sensitivity to climate implies large changes in 21st century North American forest growth. *Ecol. Lett.*, 19, 1119–1128.

Compo, G.P., Whitaker, J.S., Sardeshmukh, P.D., Matsui, N., Allan, R.J., Yin, X. *et al.* (2011). The twentieth century reanalysis project. *Q. J. R. Meteorol. Soc.*, 137, 1–28.

Cook, E. & Peters, K. (1997). Calculating unbiased tree-ring indices for the study of climatic and environmental change. *Holocene*, 7, 361–370.

D'Arrigo, R., Wilson, R., Liepert, B. & Cherubini, P. (2008). On the 'Divergence Problem' in northern forests: A review of the tree-ring evidence and possible causes. *Glob. Planet. Change*, 60, 289–305.

Dolgikh, V.I. (2006). *Phenomenon of Norilsk: History of the Norilsk industrial region*. Polar star, Moscow.

Driscoll, W., Wiles, G., D'Arrigo, R. & Wilmking, M. (2005). Divergent tree growth response to recent climatic warming, Lake Clark National Park and Preserve. *Alaska. Geophys. Res. Lett.*, 32, L20703.

Esper, J. & Frank, D. (2009). Divergence pitfalls in tree-ring research. *Clim. Change*, 94, 261–266.

Etschberger, S. & Hilbert, A. (2003). Evolutionary Strategies to Avoid Local Minima in Multidimensional Scaling. In: *Between Data Science and Applied Data Analysis* (eds Schader, M., Gaul, W., & Vichi, M.). Springer-Verlag, Berlin, Heidelberg, pp. 209–217. https://doi.org/10.1007/978-3-642-18991-3_24.

Evans, M.N., Reichert, B.K., Kaplan, A., Anchukaitis, K.J., Vaganov, E.A., Hughes, M.K. *et al.* (2006). A forward modeling approach to paleoclimatic interpretation of tree-ring data. *J. Geophys. Res. Biogeosci.*, 111, G03008.

Flanner, M.G. (2013). Arctic climate sensitivity to local black carbon. *J. Geophys. Res. Lett. A.*, 118, 1840–1851.

Fritts, H.C. (1976). *Tree Rings and Climate*. Cambridge, MA: Academic Press.

Garrett, T.J. & Verzella, L.L. (2008). An evolving history of Arctic aerosols. *Bull. American Meteor. Soci.*, 89, 299–302.

Gauthier, S., Bernier, P., Kuuluvainen, T., Shvidenko, A.Z. & Schepaschenko, D.G. (2015). Boreal forest health and global change. *Science*, 349, 819–822.

Girardin, M.P., Bouriaud, O., Hogg, T., Kurz, W.A., Zimmermann, N.E., Metsaranta, J. *et al.* (2016). No growth stimulation of Canada's boreal forest under half-century of combined warming and CO_2 fertilization. *Proc. Natl Acad. Sci. U.S.A.*, 113, E8406–E8414.

Harris, I., Jones, P.D., Osborna, T.J. & Lister, D.H. (2014). Updated high-resolution grids of monthly climatic observations – the CRU TS3.10 Dataset. *Int. J. Climatol.*, 34, 623–642.

Hirdman, D., Sodemann, H., Eckhardt, S., Burkhart, J.F., Jefferson, A., Mefford, T. *et al.* (2010). Source identification of short-lived air pollutants in the Arctic using statistical analysis of measurement data and particle dispersion model output. (2010). *Atmos. Chem. Phys.*, 10, 669–693.

Innes, J. (1987). Air Pollution and Forestry. Forestry Commission Bulletin, No. 70. Forestry Commission, HMSO Books, London.

Kharuk, V.I., Nilsson, S. & Samarskaia, E. Anthropogenic and Technogenic Stress Factors to Forests in Siberia. IIASA Working Paper WP-96-104 (1996).

Kirdyanov, A., Hughes, H., Vaganov, E., Schweingruber, F. & Silkin, P. (2003). The importance of early summer temperature and date of snow melt for tree growth in Siberian Subarctic. *Trees*, 17, 61–69.

Kirdyanov, A.V., Myglan, V.S., Pimenov, A.V., Knorre, A.A., Ekarta, A.K. & Vaganova, E.A. (2014). Die-off dynamics of Siberian larch under the impact of pollutants emitted by Norilsk enterprises. *Contemp. Probl. Ecol.*, 7, 679–684.

Kirdyanov, A.V., Saurer, M., Siegwolf, R., Knorre, A.A., Prokushkin, A.S., Churakova (Sidorova), O.V. *et al.* (2020). Long-term ecological consequences of forest fires in the continuous permafrost zone of Siberia. *Environ. Res. Lett.*, 15, 034061.

Kloeppel, B.D., Gower, S.T., Treichel, I.W. & Kharuk, S. (1998). Foliar carbon isotope discrimination in *Larix* species and sympatric evergreen conifers: A global comparison. *Oecologia*, 114, 153–159.

Knorre, A.A., Kirdyanov, A.V. & Vaganov, E.A. (2006). Climatically-induced interannual variation in aboveground biomass productivity in the forest-tundra and northern taiga of central Siberia. *Oecologia*, 147, 86–95.

Knorre, A.A., Kirdyanov, A.V., Prokushkin, A.S. & Büntgen, U. (2019). Tree ring-based reconstruction of the long-term influence of wildfires on permafrost active layer dynamics in Central Siberia. *Sci. Total Environ.*, 652, 314–319.

Korets, M.A., Ryzhkova, V.A. & Danilova, I.V. (2014). GIS-Based approaches to the assessment of the state of terrestrial ecosystems in the Norilsk industrial region. *Contemp. Probl. Ecol.*, 7, 643–653.

Law, K.S. & Stohl, A. (2007). Arctic air pollution: origins and impacts. *Science*, 315, 1537–1540.

Lewis, J. (1990). The spirit of the first Earth Day. *EPA J.*, 16, 8–12.

Lihavainen, J., Ahonen, V., Keski-Saari, S., Kontunen-Soppela, S., Oksanen, E. & Keinänen, M. (2016). Low vapour pressure deficit affects nitrogen nutrition and foliar metabolites in silver birch. *J. Exp. Bot.*, 67, 4353–4365.

Lloyd, A. & Bunn, A. (2007). Responses of the circumpolar boreal forest to 20th century climate variability. *Environ. Res Lett.*, 2, 045013.

Malavelle, F.F., Haywood, M., Jones, A., Gettelman, A., Clarisse, L., Bauduin, S. *et al.* (2017). Strong constraints on aerosol-cloud interactions from volcanic eruptions. *Nature*, 546, 485–491.

McConnell, J.R., Edwards, R., Kok, G.L., Flanner, M.G., Zender, C.S., Saltzman, E.S. *et al.* (2007). 20th-century industrial black carbon emissions altered Arctic climate forcing. *Science*, 317, 1381–1384.

Ministry of Ecology and Environmental Management of the Krasnoyarsk region (2019). *The Governmental report on the state and protection of the environment in Krasnoyarsk region in 2018*. Polygraph-Avanta Ltd., Krasnoyarsk.

Miranda, V. & Chaphekar, M. (1980). SEM study of the inner periclinal surface of leaf cuticles in the family Pinaceae. *Bot. J. Linn. Soc.*, 81, 61–78.

Najafi, M.R., Zwiers, F.W. & Gillett, N.P. (2015). Attribution of Arctic temperature change to greenhouse-gas and aerosol influences. *Nat. Clim. Change*, 5, 246–249.

Panyushkina, I.P., Shishov, V.V., Grachev, A.M., Knorre, A.A., Kirdyanov, A.V., Leavitt, S.W. *et al.* (2016). Trends in elemental concentrations of tree rings from the Siberian Arctic. *Tree Ring Res.*, 72, 67–77.

Pisaric, M.F.J., Carey, S.K., Kokelj, S.V. & Youngblut, D. (2007). Anomalous 20th century tree growth, Mackenzie Delta, Northwest Territories. *Canada. Geophys. Res. Lett.*, 34, L05714.

Ponmarev, E.I., Shvetsov, E.G. & Kharuk, V.I. (2018). The intensity of wildfires in fire emissions estimates. *Russ. J. Ecol.*, 49, 492–499.

Price, K., Storn, R.M. & Lampinen, J.A. (2005). *Differential Evolution*. A Practical Approach to Global Optimization, Natural Computing Series, Springer, Berlin Heidelberg.

Quinn, P.K., Shaw, G., Andrews, E., Dutton, E.G., Ruoho-Airola, T. & Long, S.L. (2007). Arctic haze: current trends and knowledge gaps. *Tellus B*, 59, 99–114.

Ramanathan, V., Crutzen, P.J., Kiehl, J.T. & Rosenfeld, D. (2001). Aerosol, climate and the hydrological cycle. *Science*, 294, 2119–2124.

Rinke, A., Dethloff, K. & Fortmann, M. (2004). Regional climate effects of Arctic haze. *Geophys. Res. Let.*, 31, L16202.

Roderick, M.L. & Farquhar, G.D. (2002). The cause of decreased pan evaporation over the past 50 years. *Science*, 298, 1410–1411.

Shevchenko, V., Lisitsin, A., Vinogradova, A. & Stein, R. (2003). Heavy metals in aerosols over the seas of the Russian Arctic. *Sci. Total Environ.*, 306, 11–25.

Shindell, D. (2007). Local and remote contributions to Arctic warming. *Geophys. Res. Let.*, 34, L14704.

Shvetsov, E.G., Kukavskaya, E.A., Buryak, L.V. & Barrett, K. (2019). Assessment of post-fire vegetation recovery in Southern Siberia using remote sensing observations. *Environ. Res. Lett.*, 14, 055001.

Siccama, T.G., Bliss, M. & Vogelmann, H.W. (1982). Decline of red spruce in the Green Mountains of Vermont. *Bull. Torrey Bot. Club*, 109, 162–168.

Smith, K.T., Čufar, K. & Levanič, T. (1999). Temporal stability and dendroclimatology in silver fir and red spruce. *Phyton [Austria]*, 39, 117–122.

Smith, S.J., van Aardenne, J., Klimont, Z., Andres, R.J., Volke, A. & Delgado, A.S. (2011). Anthropogenic sulfur dioxide emissions: 1850–2005. *Atmos. Chem. Phys.*, 11, 1101–1116.

Stanhill, G. (2005). Global dimming: A new aspect of climate change. *Weather*, 60, 11–14.

Stine, A.R. & Huybers, P. (2014). Arctic tree rings as recorders of variations in light availability. *Nat. Commun.*, 5, 3836.

Stohl, A. (2006). Characteristics of atmospheric transport into the Arctic troposphere. *J. Geophys. Res. Atmos.*, 111, D11306.

Stohl, A., Klimont, Z., Eckhardt, S., Kupiainen, K., Shevchenko, V.P., Kopeikin, V.M. *et al.* (2013). Black carbon in the Arctic: The underestimated role of gas flaring and residential combustion emissions. *Atmos. Chem. Phys.*, 13, 8833–8855.

Storn, R. & Price, K. (1997). Differential evolution - a simple and efficient heuristic for global optimization over continuous spaces. *J. Glob. Optim.*, 11, 341–359.

Taylor, P.C., Kato, S., Xu, K.-M. & Cai, M. (2015). Covariance between Arctic sea ice and clouds within atmospheric state regimes at the satellite footprint level. *J. Geophys. Res. Atmos.*, 120(24), 12656–12678.https://doi.org/10.1002/2015JD023520.

Telyatnikov, M.Y. & Prystyazhnyuk, S.A. (2014). Anthropogenous influence of Norilsk industrial area on plant vegetation cover of the tundra and forest tundra. *Contemp. Probl. Ecol.*, 7, 654–668.

Tolwinski-Ward, S.E., Evans, M.N., Hughes, M.K. & Anchukaitis, K.J. (2011). An efficient forward model of the climate controls on interannual variation in tree-ring width. *Clim. Dyn.*, 36, 2419–2439.

Tolwinski-Ward, S.E., Anchukaitis, K.J. & Evans, M.N. (2013). Bayesian parameter estimation and interpretation for an intermediate model of tree-ring width. *Clim. Past*, 9, 1481–1493.

Trenberth, K.E. & Fasullo, J.T. (2009). Global warming due to increasing absorbed solar radiation. *Geophys. Res. Lett.*, 36, L07706.

Twomey, S. (1977). The influence of pollution on the shortwave albedo of clouds. *J. Atmos. Sci.*, 34, 1149–1952.

Tychkov, I.I., Sviderskaya, I.V., Babushkina, E.A., Popkova, M.I., Vaganov, E.A. & Shishov, V.V. (2019). How can the parameterization of a process-based model help us understand real tree-ring growth? *Trees*, 33, 345–357.

Vaganov, E.A., Shiyatov, S.G. & Mazepa, V.S. (1996). *Dendroclimatic Investigation in Ural-Siberian Subarctic*. Nauka, Novosibirsk.

Vaganov, E.A., Hughes, M.K., Kirdyanov, A.V., Schweingruber, F.H. & Silkin, P.P. (1999). Influence of snowfall and melt timing on tree growth in subarctic Eurasia. *Nature*, 400, 149–151.

Vaganov, E. A., Hughes, M. K. & Shashkin, A.V. (2006). *Growth Dynamics of Conifer Tree Rings: Images of Past and Future Environments*. Springer, Berlin, Heidelberg.

Vaganov, E.A., Anchukaitis, K.J. & Evans, M.N. (2011). How well understood are the processes that create dendroclimatic records? A mechanistic model of the climatic control on conifer tree-ring growth dynamics. In: *Dendroclimatology* (eds Hughes, M.K., Swetnam, T.W. & Diaz, H. F.). Springer, Amsterdam, pp. 37–75. 10.1007/978-1-4020-5725-0_3.

Wang, K. & Dickinson, R.E. (2013). Contribution of solar radiation to decadal temperature variability over land. *Proc. Natl Acad. Sci. USA*, 110, 14877–14882.

Wieser, G., Hecke, K., Tausz, M. & Matyssek, R. (2013). Foliage type specific susceptibility to ozone in *Picea abies*, *Pinus cembra* and *Larix decidua* at treeline: A synthesis. *Environ. Exp. Bot.*, 90, 4–11.

Wild, M., Ohmura, A. & Makowski, K. (2007). Impact of global dimming and brightening on global warming. *Geophys. Res. Lett.*, 34, L04702.

Wild, M. (2009). Global dimming and brightening: A review. *J. Geophys. Res. Atmos.*, 114, D00D162009.

Wild, M. (2016). Decadal changes in radiative fluxes at land and ocean surfaces and their relevance for global warming *WIREs Clim. Change*, 7, 91–107.

Wild, M., Ohmura, A., Schär, C., Müller, G., Folini, D., Schwarz, M. *et al.* (2017). The Global Energy Balance Archive (GEBA) version 2017: a database for worldwide measured surface energy fluxes. *Earth Syst. Sci. Data*, 9, 601–613.

Wilmking, M., D'Arrigo, R., Jacoby, G. & Juday, G. (2005). Divergent growth responses in circumpolar boreal forests. *Geophys. Res. Lett.*, 32, L15715.

Zhao, C. & Garrett, T.J. (2015). Effects of Arctic haze on surface cloud radiative forcing. *Geophys. Res. Let.*, 42, 557–564.

Zhulidov, A.V., Robarts, R.D., Pavlov, D.F., Kämäri, J., Gurtovaya, T.Y., Meriläinen, J.J. *et al.* (2011). Long-term changes of heavy metal and sulphur concentrations in ecosystems of the Taymyr Peninsula (Russian Federation) north of the Norilsk industrial complex. *Environ. Monit. Assess.*, 181, 539–553.

Zubareva, O.N., Skripal'shchikova, L.N., Greshilova, N.V. & Kharuk, V.I. (2003). Zoning of landscapes exposed to technogenic emissions from the Norilsk mining and smelting works. *Russ. J. Ecol.*, 34, 375–380.

SUPPORTING INFORMATION

Additional supporting information may be found online in the Supporting Information section at the end of the article.